PCCP

ROYAL SOCIETY OF CHEMISTRY

PAPER

View Article Online
View Journal | View Issue

Cite this: *Phys. Chem. Chem. Phys.*, 2021, **23**, 17271

Selection rule for Raman spectra of two-dimensional materials using circularly-polarized vortex light

Riichiro Saito, *[a] Muhammad Shoufie Ukhtary, [ab] Sake Wang [a] and Nguyen Tuan Hung [c]

Received 19th May 2021,
Accepted 13th July 2021

DOI: 10.1039/d1cp02209a

rsc.li/pccp

Conservation of spin and orbital angular momenta of circularly-polarized vortex light is discussed for Raman spectra of two-dimensional materials. We first show the selection rule for optical absorption of two-dimensional materials as a function of the spin and orbital angular momentum of incident vortex light. In the case of two-dimensional materials, the Raman tensor for the incident vortex light does not change the symmetry of the phonon mode. Furthermore, the Raman active modes are classified by either "helicity-changing" or "helicity-conserved" Raman modes, in which the scattered photon of circularly polarized light either changes or does not change the helicity of the light, respectively. We show tables of selection rules for the Raman active modes of two-dimensional materials with 2, 3, 4, and 6 rotational symmetry for vortex light.

1 Introduction

Vortex light is an electro-magnetic wave (EM) with an orbital angular momentum. Vortex light has received a lot of attention due to its potential applications in areas such as quantum information protocols and optical communications.[1,2] In 1966, Kogelnik and Li derived the Laguerre–Gaussian mode of the vortex light by solving the paraxial Helmholtz equation in which the amplitude of the EM changes slowly compared with the wavelength as the wave propagates.[3] The amplitude of the ℓth Laguerre-Gaussian mode has an azimuthal phase shift term, $\exp(i\ell\varphi)$, where φ is the azimuthal angle in the cylindrical coordinate and the integer ℓ is called the topological charge. The corresponding vortex light has an orbital angular momentum $\ell\hbar$.[4] In this paper, we discuss the conservation law of angular momentum in the Raman scattering of two-dimensional (2D) materials.

For vortex light, we have another freedom of spin-angular-momentum $\pm\hbar$ depending on the left-handed ($+\hbar$) or right-handed ($-\hbar$) circularly polarized light, or the helicity of the photon (±1), which was observed experimentally by Beth in 1936.[5] Since the spin and orbital angular momenta are related to the amplitude and the phase of EM, respectively, the spin and orbital angular momenta of light are independent of each other. In previous work, we have shown the conservation law of spin-angular-momentum of circularly polarized light in the Raman spectroscopy for 2D materials that have rotational symmetry.[6] We have shown that the inelastically scattered light either changes or conserves the helicity of the incident photon, which depends on the Raman-active phonon mode and the rotational symmetry of 2D materials. The prediction of the helicity-changing Raman mode is consistent with the analysis of the Raman tensor and the Raman measurement using circularly polarized light for graphene (6-fold),[7] TaP or LaAlSi (4-fold),[8,9] transition-metal dichalcogenides (TMDs) (3-fold),[10] and ReS_2 (2-fold)[11] 2D materials. In this paper, we consider the angular momentum of the vortex light for discussing the selection rule for Raman active modes of 2D materials. Although we do not evaluate the Raman intensity, we discuss the selection rule for Raman spectra by using the incident vortex light.

Raman spectroscopy has been frequently used as a non-contact characterization technique for low-dimensional materials such as carbon nanotubes and 2D materials under ambient conditions, that is, room temperature and atmospheric pressure.[12,13] Chen *et al.* observed Raman spectra of 2D MoS_2 by using circularly-polarized light.[10] They showed that the scattered light by the in-plane E'-symmetry phonon changes the helicity of the incident circularly-polarized light as is known as helicity-changing Raman spectra, while the scattered light by the out-of-plane A_1'-symmetry phonon does not change the helicity (helicity-conserved Raman spectra). Occurrence of the helicity-changing Raman spectra is simply understood by the Raman tensor for a given phonon mode using the Jones vector of circularly-polarized light.[6]

Tatsumi *et al.* have discussed the helicity-changing Raman spectra using the conservation law of angular momentum in

[a] *Department of Physics, Tohoku University, Sendai 980-8578, Japan. E-mail: rsaito@flex.phys.tohoku.ac.jp*
[b] *Research Center for Physics, Indonesian Institute of Sciences (LIPI), Tangerang Selatan 15314, Indonesia*
[c] *Frontier Research Institute for Interdisciplinary Sciences, Tohoku University, Sendai 980-8578, Japan*

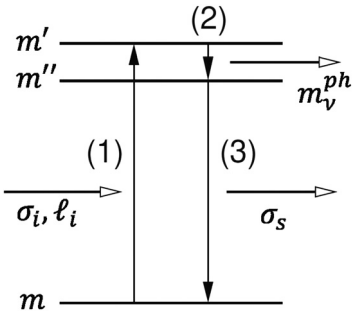

Fig. 1 Illustration of the Raman process. The first-order Raman process for emitting a phonon consists of (1) optical absorption from the m to m' electronic state by electron–photon interaction, (2) the photo-excited electron emits a phonon by the electron–phonon interaction with transition from the m' to m'' state, and (3) the photo-excited electron recombines with a hole by emitting the scattered photon by the electron–phonon interaction with transition from the m'' to m state.[12,18]

the Raman scattering process.[6] They have predicted several helicity-changing Raman active modes of 2D materials with 2, 3, 4, or 6 fold rotational symmetry around the axis perpendicular to the 2D material, which is consistent with the calculated resonant-Raman spectra[14] and the experiments.[7,10] In the first-order Raman process, we have three Raman sub-processes (see Fig. 1): (1) optical absorption of an incident photon, (2) a phonon emission by the photo-excited electron, and (3) a photon emission as the inelastic-scattered light. Each sub-process is given by the matrix elements of electron–photon (1, 3) and electron–phonon (2) interactions. When a 2D material has an N-fold rotational symmetry and when the ν-th phonon has an N_ν-fold rotational symmetry, the electron–photon and electron–phonon matrix elements have the optical selection rules by the N-fold and N_ν-fold rotational symmetry, respectively, whose products give the conservation law of angular momentum of the materials.[6] This concept can be extended to the angular momentum of the vortex light, which is the motivation of the present paper.

Ishii *et al.*[15] discussed the optical selection rule for optical absorption of the vortex light for monolayer MoS_2 with a 3-fold rotational symmetry, in which they showed that the orbital angular momentum gives the valley-dependent selection rule at the K and K' points in the hexagonal Brillouin zone. Li *et al.*[16] discussed the Raman scattering of 3D cubic material using the vortex light in which they assumed that orbital angular momentum is not coupled with the materials but that the Raman tensor changed the form as a function of the orbital angular momentum which results in the appearance of a new Raman-active mode as a function of orbital angular momentum in the case of 3D materials. Here we explain that the shape of the Raman tensor does not change for vortex light in the case of 2D materials.

The organization of the paper is as follows. In Section 2, we discuss how to obtain the conservation of angular momentum. In Section 3, we show the selection rules of electron–photon and electron–phonon matrix elements in the Raman scattering. In Section 4, we calculate the conservation law in Raman scattering for two-dimensional materials with 2, 3, 4, and 6 rotational symmetry. In Section 5, the main results of the conservation law are tabulated, followed by discussion and summary.

2 Conservation law of angular momentum

Here, we consider a 2D material that has N-fold rotational symmetry around the z axis perpendicular to the material in the xy plane. Hereafter, we consider the case where the incident and scattered light propagates in the directions of $-z$ and $+z$, respectively. Let us define the rotation operator around the z axis with an angle $\alpha = 2\pi/N$ as follows:

$$\mathscr{U}(\alpha) = \exp\left(-i\frac{\alpha L_z}{\hbar}\right), \tag{1}$$

where $L_z \equiv -i\hbar\partial/\partial\varphi$ is the z component of the angular momentum operator in a cylindrical coordinate. Since the Hamiltonian $\mathscr{H}$ is commutable with $\mathscr{U}(\alpha)$, $[\mathscr{H}, \mathscr{U}(\alpha)] = 0$, any wavefunction of $\mathscr{H}$, $|m\rangle$, is also an eigenfunction of $\mathscr{U}(\alpha)$, that is, $\mathscr{U}(\alpha)|m\rangle = C|m\rangle$. Using the facts that $\{\mathscr{U}(\alpha)\}^N$ is a 2π rotation and that $C^N = 1$, the eigenvalues of $\mathscr{U}(\alpha)$ are expressed by,

$$\mathscr{U}(\alpha)|m\rangle = \exp(-im\alpha)|m\rangle, \quad (m = 0, 1, 2, \ldots, N-1) \tag{2}$$

When we consider the cylindrical coordinate, the eigenfunction of L_z is given by $\exp(im\varphi)$ whose eigenvalue is $m\hbar$. When we multiply $\mathscr{U}(\alpha)$ by $\exp(im\varphi)$, we get

$$\begin{aligned}\mathscr{U}(\alpha)\exp(im\varphi) &= \exp\{im(\varphi-\alpha)\}\\ &= \exp(-im\alpha)\exp(im\varphi),\end{aligned} \tag{3}$$

which means that $\exp(im\varphi)$ is an eigenfunction of $\mathscr{U}(\alpha)$ for the eigenvalue of $\exp(-im\alpha)$. Thus it is reasonable for us to call $m\hbar$ a pseudo angular momentum though the definition is valid only for a discrete rotational angle.

Let us consider how to rotate a matrix element, $\langle m'|\mathscr{O}|m\rangle$ by $\mathscr{U}(\alpha)$ for an interaction operator $\hat{\mathscr{O}}$ which has an N'-fold rotational symmetry. In general, the value of N' is smaller than N. However, if $\mathscr{O}$ does not depend on φ, N' becomes infinite. In this case, we can select as $N' = N$. When we operate $\mathscr{U}(\alpha)$ on $\mathscr{O}$, the variable φ in $\mathscr{O}$ is changed to $\varphi + \alpha$. If the $\mathscr{O}$ has a φ dependence as $\exp(im_O\varphi)$, we obtain

$$\mathscr{O}(\varphi + \alpha) = \exp(-im_O\alpha)\mathscr{O}(\varphi), \tag{4}$$

where an integer m_O is taken from $m_O = 0, 1, \ldots, N' - 1$ which satisfies $\mathscr{O}(\varphi + 2\pi) = \mathscr{O}(\varphi)$.

When we apply $\mathscr{U}(\alpha)$ to $\mathscr{O}(\varphi)$, we get

$$\mathscr{U}(\alpha)\mathscr{O}(\varphi) = \mathscr{O}(\varphi + \alpha)\mathscr{U}(\varphi) = \exp(-im_O\alpha)\mathscr{O}(\varphi)\mathscr{U}(\alpha), \tag{5}$$

from which we obtain the unitary transformation of $\mathscr{O}(\varphi)$ as follows

$$\mathscr{U}(\alpha)\mathscr{O}\mathscr{U}^{-1}(\alpha) = \exp(-im_O\alpha)\mathscr{O}. \tag{6}$$

Using eqn (2) and (6), when we rotate the matrix element, $\langle m'|\mathscr{O}|m\rangle$, we get

$$\begin{aligned}&\langle m'|\mathscr{U}^{-1}(\alpha)\mathscr{U}(\alpha)\mathscr{O}\mathscr{U}^{-1}(\alpha)\mathscr{U}(\alpha)|m\rangle\\ &= \exp\{i(-m + m' - m_O)\alpha\}\langle m'|\mathscr{O}|m\rangle.\end{aligned} \tag{7}$$

It is noted that $\mathscr{O}$ generally has a lower symmetry than $\mathscr{H}$ and that α in $\mathscr{U}(\alpha)$ should be selected for the N'-fold rotational symmetry. Here we assume that N' is a divisor of N. If the matrix elements of $\mathscr{O}$ have an N'-fold rotational symmetry, the $\exp i(m - m' + m_O)\alpha$ should be unity, in which m and m' (or m_O) are integers from 0 to $N' - 1$. Otherwise, by integration of the matrix elements over the φ from 0 to 2π, the integration would give zero. From this fact, we get the conservation law of angular momentum as follows

$$m' - m - m_O = N'p, \tag{8}$$

where p is any integer. Eqn (8) is understood by the conservation law of angular momentum for the operator $\mathscr{O}$.

In the next section we consider the selection rule for electron–photon and electron–phonon matrix elements using eqn (8).

3 Selection rule of the matrix element

3.1 Electron–photon matrix element

The electron–photon matrix element $\mathscr{M}_{opt}$ is given by time-dependent perturbation theory as follows[17]

$$\mathscr{M}_{opt} = \frac{ie\hbar}{m_e}\langle m'|\boldsymbol{A}_\ell^\sigma \cdot \nabla|m\rangle, \tag{9}$$

where m_e is the mass of an electron and $\boldsymbol{A}_\ell^\sigma$ is the vector potential of the light. For the Laguerre–Gaussian mode of the vortex light, the vector potential in the cylindrical coordinate is given by[15]

$$\begin{aligned}\boldsymbol{A}_\ell^\sigma(r,\varphi,z) &= \boldsymbol{e}_A^\sigma\sqrt{\frac{2p!}{\pi(p+|\ell|)!}}\frac{w_0}{w(z)}\left(\frac{\sqrt{2}r}{w(z)}\right)^{|\ell|}L_p^{|\ell|}\left(\frac{2r^2}{w^2(z)}\right)\\ &\quad\times\exp\left(-\frac{r^2}{w^2(z)}\right)\exp(i\ell\varphi - i\omega t + ikz)\\ &\equiv \boldsymbol{e}_A^\sigma f(r,z)\exp(i\ell\varphi),\end{aligned} \tag{10}$$

where ℓ, p, z, r, $L_p^{|\ell|}$, w_0, and $w(z)$ denote, respectively, orbital angular momentum, the radial index, propagation direction (z) and radial direction (r) in the cylindrical coordinate, the Laguerre polynomial function, the beam waist and the beam width function. $\boldsymbol{e}_A^\sigma$ is the unit vector for the amplitude of light, which is known as the Jones vector,

$$\boldsymbol{e}_A^\sigma = \frac{1}{\sqrt{2}}\begin{pmatrix}1\\ i\sigma\end{pmatrix}, \tag{11}$$

where $\sigma = +1$ and $\sigma = -1$ denote the spin-angular momentum of the light, and correspond to the left-handed and right-handed circularly polarized light (LCP and RCP), respectively. The function $f(r, z)$ in eqn (10) is defined as the remaining part of $\boldsymbol{A}_\ell^\sigma$ except for the factors of $\boldsymbol{e}_A^\sigma$ and $\exp(i\ell\varphi)$. We will use the fact that the $f(r, z)$ does not contain φ.

The optical transition is allowed when $\mathscr{M}_{opt} \neq 0$, while the transition is forbidden when $\mathscr{M}_{opt} = 0$. When we multiply $\mathscr{U}^{-1}(\alpha)\mathscr{U}(\alpha)$ in eqn (9), we obtain the following expression, by putting eqn (10) into eqn (9).

$$\begin{aligned}\mathscr{M}_{opt} &= \langle m'|\exp(i\ell\varphi)f(r,z)\boldsymbol{e}_A^\sigma\cdot\nabla|m\rangle,\\ &= \langle m'|\exp(i\ell\varphi)f(r,z)\mathscr{U}^{-1}(\alpha)\\ &\quad\times\mathscr{U}(\alpha)\boldsymbol{e}_A^\sigma\mathscr{U}^{-1}(\alpha)\cdot\mathscr{U}(\alpha)\nabla\mathscr{U}^{-1}(\alpha)\mathscr{U}(\alpha)|m\rangle,\end{aligned} \tag{12}$$

where ∇ corresponds to $\mathscr{O}$ in eqn (7). Since $f(r, z)$ does not contain φ, and since $\boldsymbol{e}_A^\sigma$ is commutable[6] with $\mathscr{U}(\alpha)$, that is, $\mathscr{U}(\alpha)\boldsymbol{e}_A^\sigma\mathscr{U}^{-1}(\alpha) = \boldsymbol{e}_A^\sigma$, the left-most $\mathscr{U}^{-1}(\alpha)$ in eqn (12) applies to the product of the functions, $\langle m'|\exp(i\ell\varphi)$ from the right as follows

$$\langle m'|\exp(i\ell\varphi)\mathscr{U}^{-1}(\alpha) = \exp\{i(m' - \ell)\alpha\}\langle m'|\exp(i\ell\varphi). \tag{13}$$

In eqn (13), we use eqn (3) for $\exp(i\ell\varphi)$ as follows,

$$\mathscr{U}(\alpha)\exp(i\ell\varphi) = \exp(-i\ell\alpha)\exp(i\ell\varphi). \tag{14}$$

For the inner product of $\boldsymbol{e}_A^\sigma\cdot\{\mathscr{U}(\alpha)\nabla\mathscr{U}^{-1}(\alpha)\}$, we get as follows,[6]

$$\begin{aligned}&\boldsymbol{e}_A^\sigma\cdot\left\{\mathscr{U}(\alpha)\nabla\mathscr{U}^{-1}(\alpha)\right\}\\ &= \frac{1}{\sqrt{2}}\begin{pmatrix}1 & -i\sigma\end{pmatrix}\begin{pmatrix}\cos\alpha & -\sin\alpha\\ \sin\alpha & \cos\alpha\end{pmatrix}\begin{pmatrix}\frac{\partial}{\partial x}\\ \frac{\partial}{\partial y}\end{pmatrix}\\ &= \frac{1}{\sqrt{2}}\left((\cos\alpha - i\sigma\sin\alpha)\frac{\partial}{\partial x} - i\sigma(\cos\alpha - i\sigma\sin\alpha)\frac{\partial}{\partial y}\right)\\ &= \frac{1}{\sqrt{2}}\exp(-i\sigma\alpha)\left(\frac{\partial}{\partial x} - i\sigma\frac{\partial}{\partial y}\right)\\ &= \exp(-i\sigma\alpha)(\boldsymbol{e}_A^\sigma\cdot\nabla),\end{aligned} \tag{15}$$

where we use the relation that $\exp(-i\sigma\alpha) = \cos\alpha - i\sigma\sin\alpha$, for $\sigma = \pm 1$.

Using eqn (10), (12), (13) and (15), eqn (12) becomes

$$\mathscr{M}_{opt} = \exp\{i(m' - m - \sigma - \ell)\alpha\}\langle m'|\boldsymbol{A}_\ell^\sigma\cdot\nabla|m\rangle. \tag{16}$$

Since eqn (9) and (12) are identical, we get the following selection rule for the vortex light from eqn (16)

$$m' - m - \sigma - \ell = Np, \tag{17}$$

where p is any integer. In particular, if eqn (17) does not satisfy, $\mathscr{M}_{opt}$ should be zero. It is important to note that both σ and ℓ can be either a positive or negative integer. Although we have the expression of $-\sigma - \ell$, we have any combination of σ and ℓ with a positive or negative integer.

3.2 Electron–phonon matrix element

The electron–phonon matrix element $\mathscr{M}_{ep}$ is given by

$$\mathscr{M}_{ep} = \langle m''|\boldsymbol{A}_\nu\cdot\nabla V|m'\rangle, \tag{18}$$

where $\boldsymbol{A}_\nu$ and ∇V denote, respectively, the amplitude of the ν-th phonon mode and deformation potential. Tatsumi *et al.* give the selection rule for $\mathscr{M}_{ep}$,[6] which is common for the Raman spectra for non-vortex light as follows.

$$m'' - m' = -m_\nu^{ph} + N_\nu p_2, \tag{19}$$

where p_2 is any integer, m_ν^{ph} is an angular momentum of the ν-th phonon, and N_ν is an integer for the N_ν-th rotational symmetry for the ν-th phonon. For example, in a TMD which has a three-fold rotational symmetry and thus $N = 3$, Tatsumi *et al.* gave $N_\nu = N = 3$ or $N_\nu = 1$ for the A_1' and the E' Raman active modes, respectively.[6]

It is important to comment on the treatment of the N_ν. A phonon eigen-mode at the Γ point in the Brillouin zone belongs to the irreducible representation of the point group of the unit cell. For the Raman active modes, the phonon oscillation behaves as a quadratic function for the irreducible representation such as $x^2 - y^2$ or xy from which we can make the Raman tensor. The linear combination of these functions can be an eigenfunction of $\mathscr{U}(\alpha)$ for N (not N_ν) rotational symmetry. For example, the E' mode ($x^2 - y^2$, xy) of TMD, which was given by $N_\nu = 1$ and $m_\nu^{\mathrm{ph}} = 0$,[6] can be expressed by $N_\nu = N = 3$ and $m_\nu^{\mathrm{ph}} = \pm 2$. In fact, when we multiply $\mathscr{U}(\alpha)$ with $\alpha = 2\pi/3$ by $(x^2 - y^2 \pm i2xy)$, we get

$$\mathscr{U}\left(\frac{2\pi}{3}\right)(x^2 - y^2 \pm i2xy) = \exp\left(\mp\frac{4\pi i}{3}\right)(x^2 - y^2 \pm i2xy). \quad (20)$$

Eqn (20) means that the phonon amplitude for the E' mode is expressed by the linear combination of eigenstate of $\mathscr{U}(\alpha)$ with $m_\nu^{\mathrm{ph}} = \pm 2$. Since we have several possible m_ν^{ph} for one phonon mode, we need to consider eqn (19) for each value of m_ν^{ph}.

We think that the new expression of m_ν^{ph} is reasonable for $\ell_i \neq 0$, though both expressions give almost the same results for $\ell_i = 0$. In order to avoid any confusion between the notations by Tatsumi *et al.* and those in the present paper, we keep using eqn (19) but hereafter we set $N_\nu = N$ and we use the new value of m_ν^{ph}.

3.3 Raman process

In Fig. 1, we illustrate the first-order Raman process for emitting a phonon which consists of (1) optical absorption from the m to m' electronic states by the electron–photon interaction, (2) the photo-excited electron emits a phonon by the electron–phonon interaction with transition from the m' to m'' state, and (3) the photo-excited electron recombines with a hole by emitting the scattered photon by the electro–phonon interaction with transition from the m'' to m state.[12,18] For (1) and (2), the optical selection rules of eqn (17) and (19) are applied, respectively, to get the selection rule for each sub-process.

For the absorption sub-process (1), we get the conservation rule from eqn (17)

$$m' - m = \sigma_i + \ell_i + Np_1, \quad (p_1 = 0, \pm 1, \pm 2, \ldots), \quad (21)$$

where σ_i and ℓ_i denote the spin and orbital quantum numbers of the incident light, respectively. For the phonon emission sub-process (2), we get the conservation rule from eqn (19)

$$m'' - m' = -m_\nu^{\mathrm{ph}} + N_\nu p_2, \quad (p_2 = 0, \pm 1, \pm 2, \ldots). \quad (22)$$

For the optical transition to the bottom of the conduction band, since the m'' state is a virtual state that is given by a linear combination of excited states in perturbation theory, we usually approximate as $m'' = m'$. However, it is noted that we can take many possible values of m'' in eqn (22) in the selection rule, since the intermediate state for m'' is a virtual state. For the scattered photon emission sub-process (3), the matrix element is the complex conjugate of that for absorption. Then, we get the conservation rule without ℓ from eqn (17) as follows

$$m - m'' = -\sigma_s + Np_3, \quad (p_3 = 0, \pm 1, \pm 2, \ldots), \quad (23)$$

where σ_s denotes the spin quantum numbers of the scattered light. Here, we assume that the scattered light does not have orbital angular momentum. The assumption is reasonable since the generation of the angular momentum in vortex light does not come from the dipole transition of electron but from some optical techniques such as spiral phase plate[19] *etc.* By adding each side of eqn (21)–(23), we get the conservation rule for the Raman process as follows;

$$\sigma_s - \sigma_i - \ell_i = -m_\nu^{\mathrm{ph}} + N_\nu p, \quad (p = 0, \pm 1, \pm 2, \ldots) \quad (24)$$

where we adopt $N_\nu = N$ as discussed in Section 3.2. Since eqn (24) does not contain m, m' and m'', the final result does not depend on the quantum number of the wavefunction. This does not mean that the optical selection rule for Raman scattering does not contain the information of wavefunction. When one of the three matrix elements in the Raman process becomes zero by eqn (21)–(23), the Raman-scattering amplitude becomes zero. Thus, we need to consider each optical selection rule for the Raman process. When we put $\ell_i = 0$, the conservation rule should correspond to the case of non-vortex light that we obtained in previous work except for eqn (22).[6]

4 Examples of MoS_2 and graphene

Let us show examples of the selection rule for the Raman active modes of 2D materials with $N = 2$, 3, 4, 6 rotational symmetry. First, we discuss the transition-metal dichalcogenides, MoS_2 ($N = 3$) since the effect of rotational symmetry works not only for the Raman tensor but also the selection rule for optical absorption.

4.1 Valley polarization effect in MoS_2 with $\ell_i \neq 0$ ($N = 3$)

The monolayer, MoS_2, has a three-fold rotational symmetry ($N = 3$). It is known that the valley polarization effect for optical absorption occurs for circularly polarized light, in which the optical absorption occurs for LCP (RCP) light at the K (K') point in the hexagonal Brillouin zone.[20–27] We note here that the label of either K or K' points in the hexagonal Brillouin zone can be determined by the valley polarization effect in which we define the K (K') point by optical absorption of the LCP (RCP) light. The valley polarization corresponds to the case in eqn (21)

$$m' - m = (\sigma_i + \ell_i) + 3p_1 \quad (p_1 = 0, \pm 1, \pm 2, \ldots), \quad (25)$$

in which the value of m (m') is the eigenvalues of the 3-fold rotational symmetry for the valence (conduction) band that depends on the K or K' valleys. It is noted that the values of m

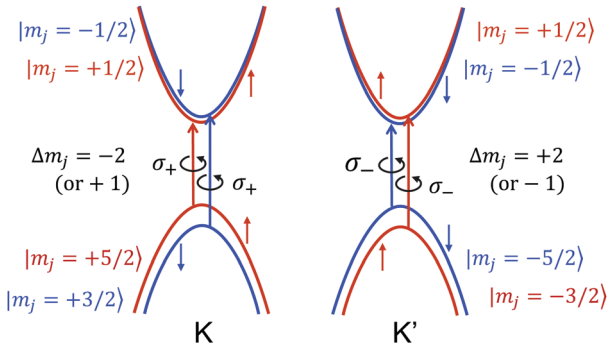

Fig. 2 The valley polarization appears in MoS_2 in which the optical absorption selectively occurs for the left-handed (or right-handed) circularly polarized light (LCP σ_+, or RCP σ_-) at the K (or K') point in the hexagonal Brillouin zone. At the K (τ = +1) and K' (τ = −1) points, the valence band consists of the $d_{x^2-y^2} + 2i\tau d_{xy}$ orbitals of Mo whose m values are +2 and −2, respectively. The conduction band consists of d_{z^2} with m = 0 at both the K and K' points. Furthermore, the valence band and conduction band are split into two spin-dependent subbands with m_j values by spin–orbit interactions. Optical dipole transition occurs between the same spin subbands with $\Delta m_j = \mp 2$ which is equivalent to $\Delta m_j = \pm 1$ in the 3-fold rotational symmetry with a non-zero p_1 value in eqn (25).

(m') give an opposite sign between K and K' valleys because of time-reversal symmetry.

In Fig. 2, we show the valence and conduction bands near the K and K' points that are split into the spin-up (red) and spin-down (blue) sub-bands by spin–orbit interactions. At the K and K' points, the valence band consists of the $d_{x^2-y^2} + 2i\tau d_{xy}$ orbital of a Mo atom in which τ is the valley index (τ = +1 for the K point and τ = −1 for the K' point).[28] The corresponding m value is 2τ. The conduction band consists of d_{z^2} with m = 0 at both the K and K' points. It is noted that the phase factor, $\exp(i\boldsymbol{k}\cdot\boldsymbol{R})$, of the Bloch wavefunction at $\boldsymbol{k} = K(K')$ point does not change the shape by operating C_3 ($\alpha = 2\pi/3$) rotation to $\boldsymbol{R}$, that is, $\exp(i\boldsymbol{k}\cdot(C_3\boldsymbol{R})) = \exp(i\boldsymbol{k}\cdot\boldsymbol{R})$. Only the atomic orbitals at each $\boldsymbol{R}$ are rotated $2\pi/3$ around $C_3\boldsymbol{R}$ by the C_3 rotation.

The half-integer values of m_j for each subband in Fig. 2 are given by summing m and $\pm 1/2$ (for up (+) and down (−) spin) by spin–orbit interactions. The dipole optical transition occurs from the valence band to the conduction band with keeping the spin direction unchanged, which gives $\Delta m_j = -2(2)$ for the $K(K')$ points. Since $\Delta m_j = -2(2)$ is equivalent to $\Delta m_j = 1(-1)$ in the 3-fold rotational symmetry by adopting non-zero p_1 in eqn (25), the left-hand side of eqn (25) can be written as follows:

$$\Delta m \equiv m' - m = \begin{cases} +1 & (K \text{ point}) \\ -1 & (K' \text{ point}) \end{cases}. \qquad (26)$$

In Table 1, we show either K or K' point at which the optical absorption occurs by showing the possible p_1 values in eqn (25). The data in Table 1 are consistent with the results shown in Table 1 by Ishii *et al.* though they did not show the derivation of the results.[15] When we consider a non-vortex light ($\ell_i = 0$), $p_1 = 0$ satisfies eqn (25) as $\Delta m = \sigma_i$, which is the origin of the valley polarization effect. When $\ell_i = -1$ and $\sigma_i = 1$ (LCP), eqn (25) is not satisfied for any p_1 for $\Delta m = -1$ (the K' point). On the other hand, for $\Delta m = 1$ (the K point), $p_1 = 1$ satisfies eqn (25) when $\ell_i = -1$ and $\sigma_i = -1$. This means that only RCP with $\ell_i = -1$ is absorbed at the K point (not the K' point) and that there is no optical absorption for LCP with $\ell_i = -1$. Similarly, when $\ell_i = +1$, only LCP is absorbed at the K' point and there is no optical absorption for RCP.

Table 1 Selection rule of optical absorption of MoS_2 for vortex light. K and K' denote that the absorption occurs at the K and K' points for LCP or RCP. Corresponding values of p_1 in eqn (25) are also listed. The symbol "—" denotes optically forbidden

ℓ_i	−3	−2	−1	0	1	2	3
LCP (σ_i = + 1)	K	K'	—	K	K'	—	K
p_1	1	0	—	0	−1	—	−1
RCP (σ_i = −1)	K'	—	K	K'	—	K	K'
p_1	1	—	1	0	—	0	−1

Thus, the optical absorption always occurs for any ℓ_i as shown in Table 1, which makes it difficult to observe the optical absorption at one valley for $\ell_i = 3p \pm 1$ (p is an integer). Since the conduction band is split by spin–orbit interactions, the lowest conduction band is spin-polarized whose direction is opposite for the K and K' points. Thus, if we can measure the spin of photo-excited carrier excited by the light with the excitation energy at the energy gap (or A exciton), we can observe whether the optical absorption occurs at the K and K' points for a given ℓ_i.

4.2 Raman selection rule of MoS_2

From eqn (24), let us obtain the selection rule for Raman spectra. In MoS_2, there are two Raman-active modes, that is, the out-of-plane chalcogen (OC) mode and the in-plane metal and chalcogen (IMC) mode which belong to A_{1g} and E_{2g} irreducible representation of D_{3h}, respectively. As is discussed in Section 3.2, we adopt $N_\nu = N$ for both the OC and IMC modes. The value of m_ν^{ph} for the OC mode is 0 while m_ν^{ph} of the IMC mode is ± 2.

When we discuss the Raman selection rule of the resonant Raman spectra by vortex light for 2D materials, we can use the following three rules: (1) conservation of angular momentum (eqn (24)), (2) optical absorption selection rule (eqn (21)) and (3) either helicity-conserved ($\sigma_i = \sigma_s$) or helicity-changing ($\sigma_i = -\sigma_s$) Raman mode. The reason why we can use rule (3) even for the vortex light is that the symmetry of the Raman tensor does not change even though we consider the function of $r = (x^2 + y^2)^{1/2}$ in the vector potential $\boldsymbol{A}$, eqn (10). Here we consider the geometry of the incident (scattered) light in the direction of $-z$ ($+z$), any function of r is invariant for a rotation around the z axis and thus the symmetry for the function of r belongs the A_{1g} symmetry. Thus, any product of (1) phonon wavefunction in an irreducible representation and (2) the function of r in the A_{1g} irreducible representation does not change the symmetry of the phonon wavefunction. As a result, the fact of either helicity-conserved ($\sigma_i = \sigma_s$) or helicity-changing ($\sigma_i = -\sigma_s$) Raman mode does not change even for $\ell_i \neq 0$. In the case of 3D material, on the other hand, since the cylindrical variable $r = (x^2 + y^2)^{1/2}$ does not belong to A_{1g} that usually belongs

Table 2 Raman selection rule of 2D MoS_2 for vortex light. For a given ℓ_i, σ_i is the possible incident LCP (σ_i = 1) and RCP (σ_i = 1) where optical absorption occurs. For each σ_i = 1 or −1, σ_s becomes either helicity-conserved or helicity-changing scattered circularly polarized light for the OC and IMC phonon modes, respectively. We expect that Raman signal might appear only when ℓ_i is a multiple of 3

ℓ_i	−3	−2	−1	0	1	2	3
σ_i	±1	+1	−1	±1	+1	−1	±1
σ_s(OC)	±1	—	—	±1	—	—	±1
σ_s(IMC)	∓1	—	—	∓1	—	—	∓1

to $r = (x^2 + y^2 + z^2)^{1/2}$ in 3D, the shape of Raman tensor depends on ℓ, which was discussed by Li *et al.*[16]

In the case of Raman spectra by non-vortex light, Chen *et al.* observed that the IMC mode ($x^2 - y^2$, xy, $m^{ph}_{IMC} = \pm 2$) is the helicity-changing Raman mode ($\Delta\sigma \equiv \sigma_i - \sigma_s = \pm 2$) while the OC mode ($x^2 + y^2$, $m^{ph}_{OC} = 0$) is helicity-conserved Raman mode ($\Delta\sigma = 0$), which is consistent in the case of $\ell_i = 0$ and the above values of N_ν and m^{ph}_ν in eqn (24).[6]

In Table 2, we list the selection rule of 2D MoS_2 for Raman spectra of the OC and IMC modes using LCP or RCP light. For a given ℓ_i, σ_i is the possible incident LCP ($\sigma_i = 1$) or RCP ($\sigma_i = -1$) light that give Raman scattering. When we put the values of $N_\nu = 3$, $\sigma_s = \sigma_i$ and $m^{ph}_{OC} = 0$ for the OC mode in eqn (23), we get $-\ell_i = 3p$. Thus, the Raman signal for OC can be observed only for $\ell_i = 3p$. When we put the values of $N_\nu = 3$, $\sigma_s = -\sigma_i$ and $m^{ph}_{IMC} = \pm 2$ for the IMC mode in eqn (23), we get $-2\sigma_i - \ell_i = \pm 2 + 3p$. For $\ell_i = 1$, since $\sigma_i = 1$, we do not have a solution for p. Similarly, for $\ell_i = -1$, since $\sigma_i = -1$, we do not have a solution for p, either. Thus, we expect that the Raman signal might appear only when ℓ_i is a multiple of 3 as listed in Table 2.

4.3 Raman selection rule for graphene (N = 6)

In the case of graphene (N = 6), the first-order Raman mode is the G band with E_{2g} symmetry ($x^2 - y^2$, xy, $m^{ph}_G = \pm 2$) of the D_{6h} point group.[6] The helicity-resolved Raman intensity of the G band is calculated[14] and is observed experimentally[7] as the helicity-changing Raman mode $\sigma_i = -\sigma_s$ for non-vortex, incident light. In the case of graphene, since there is no energy gap at the K (K') point, we cannot use the selection rule of optical absorption at the high-symmetry K (K') points. Furthermore, since the optical transition from the π to π* bands occurs for the atomic dipole moment of the $2p_z$ orbitals between the nearest-neighbor carbon atoms,[29] we cannot obtain the value of Δm for the optical absorption at a general $\boldsymbol{k}$. Thus, we generally expect optical absorption for any ℓ_i.

When we put in eqn (24) $\sigma_s - \sigma_i = \pm 2$ and $m^{ph}_G = \pm 2$, we get,

$$\pm 2 - \ell_i = \pm 2 + 6p \qquad (27)$$

In the case of $\ell_i = 0$, we have a solution $p = 0$ in eqn (27). When ℓ_i is an odd number, we do not have a solution of p in eqn (27) and thus we do not expect a Raman signal of the G band for odd numbers of ℓ_i. For $\ell_i = 2$, if $\sigma_s - \sigma_i = -2$, we have a solution of $p = -1$ and $m^{ph}_G = +2$ in eqn (27), which correspond to the helicity changing Raman scattering from LCP to RCP. For $\ell_i = -2$, if $\sigma_s - \sigma_i = +2$, we have a solution of $p = +1$ and $m^{ph}_G = -2$ in eqn (27), which correspond to the helicity changing Raman scattering from RCP to LCP.

Table 3 Raman selection rule of graphene for vortex light. When $\ell_i = 6p$, we get Raman spectra of the G band for both the LCP and RCP incident light. When $\ell_i = 6p + 2$ (or $6p - 2$), we get Raman spectra of the G band for LCP (RCP) incident light. For odd numbers of ℓ_i, although we expect optical absorption, we do not expect G band Raman signal

ℓ_i	−4	−3	−2	−1	0	1	2	3	4
σ_i	+1	—	−1	—	±1	—	+1	—	−1
$\sigma_s(G)$	−1	—	+1	—	∓1	—	−1	—	+1

In Table 3, we show the possible σ_i for observing the G band Raman spectra. When $\ell_i = 6p$, we get Raman spectra of the G band for both the LCP and RCP incident light. When $\ell_i = 6p + 2$ (or $6p - 2$), we get Raman spectra of the G band for LCP (RCP) incident light.

4.4 Raman selection rule for 2D black phosphorus (N = 2)

2D black phosphorus has a rotational symmetry with $N = 2$.[30,31] The observed Raman active modes are two A_g (x^2 or y^2) and one B_{1g} (xy).[32] Although there are no published experimental results for helicity-dependent Raman spectra for black phosphorus, we used the theoretical result by Tatsumi *et al.*[6] in which both the A_g and B_{1g} with $N = 2$ and $N_\nu = 2$ show the helicity-changing Raman spectra for $\ell_i = 0$, which is consistent with the shape of the Raman tensor. It is noted here that the Raman tensor for A_g (x^2) consists of both helicity-changing and helicity-conserved Raman spectra since the Raman tensor for x^2 can be expressed by the sum of $x^2 - y^2$ and $x^2 + y^2$, respectively. On the other hand, the Raman tensor for B_{1g} (xy) has only the helicity-changing Raman spectra. As we discussed in the case of graphene, we get $m^{ph}_\nu = 0$ for both the A_g (x^2 or y^2) and B_{1g} (xy) modes for $N_\nu = N = 2$.

The symmetry of the wavefunction of black phosphorus, which consists of the P $3p_z$ orbitals, at the top of the valence band at the Γ point in the Brillouin zone is Γ_2^+ (B_{1g}, xy) irreducible representation of D_{2h}, while that the bottom of the conduction band belongs to Γ_4^- (B_{3u}, x).[33] Since the product of $B_{1g} \times B_{3u}$ is B_{2u}, (x^2y), the dipole transition occurs by linear polarization in the direction of y, (B_{2u}) at the Γ point in the Brillouin zone. Furthermore, since the linear polarization of y is given by subtracting LCP ($x + iy$) from RCP ($x - iy$), the optical transition is allowed for both LCP and RCP light. Thus, we assumed that $m' - m = \pm 1$ for $\sigma_i = \pm 1$ which satisfies eqn (21) with $\ell_i = 0$. In Table 4 we show σ_s for the A_g or B_{2g} modes. When ℓ_i is an odd number, optical absorption for $\sigma_i = \pm 1$ does not occur. When ℓ_i is an even number, the helicity changing Raman spectra is observed for both the LCP and RCP light. The results in Table 4 are similar to those of Table 3 except for $\sigma_s(A_g)$ that consists of both LCP and RCP.

4.5 Raman selection rule for TaP or LaAlSi (N = 4)

Finally, let us discuss 2D materials with four-fold rotational symmetry (D_{4h}, $N = 4$). Although some Weyl semi-metals such as TaP[8] or LaAlSi[9] show four-fold rotational symmetry, 2D materials of TaP or LaAlSi have not been obtained yet. The optical absorption

Table 4 Raman selection rule of 2D black phosphorus for vortex light. Here we consider helicity-conserved A_g and helicity-changing B_{2g} modes. When ℓ_i is an odd number, optical absorption for $\sigma_i = \pm 1$ does not occur. When ℓ_i is an even number, the helicity changing Raman spectra are observed for both LCP ($\sigma_i = +1$) and RCP ($\sigma_i = -1$). The label of (+1, −1) denotes that the both helicity-changing and helicity-conserved Raman spectra are observed

ℓ_i	−2	−1	0	1	2
σ_i	±1	—	±1	—	±1
$\sigma_s(B_{2g})$	∓1	—	∓1	—	∓1
$\sigma_s(A_g)$	(+1, −1)	—	(+1, −1)	—	(+1, −1)

Table 5 Selection rule for Raman spectra of $N = 4$ 2D materials for vortex light. Here we consider the A_{1g} and B_{1g} (or B_{2g}) modes for σ_s which are, respectively, helicity-conserved and helicity-changing modes. Helicity-conserved A_{1g} Raman spectra can be observed for $\ell_i = 4p$, while helicity-changing B_{1g} or B_{2g} Raman spectra can be observed for odd numbers of ℓ_i

ℓ_i	−4	−3	−2	−1	0	1	2	3	4
σ_i	±1	±1	—	±1	±1	±1	—	±1	±1
$\sigma_s(A_{1g})$	±1	—	—	—	±1	—	—	—	±1
$\sigma_s(B_{1g})$	—	∓1	—	∓1	—	∓1	—	∓1	—
$\sigma_s(B_{2g})$	—	∓1	—	∓1	—	∓1	—	∓1	—

of TaP and LaAlSi occurs at the Weyl nodes whose position is not at a high-symmetry point in the Brillouin zone. Thus, we do not expect the selection rule for optical absorption. For the D_{4h} symmetry, B_{1g} $(x^2 - y^2)$ and B_{2g} (xy) modes $\left(m^{\mathrm{ph}}_{B_{1g}} = \pm 1,\ m^{\mathrm{ph}}_{B_{2g}} = \pm 1\right)$ are helicity-changing Raman modes while A_{1g} $(x^2 + y^2,\ m^{\mathrm{ph}}_{A_{1g}} = 0)$ is the helicity-conserved Raman mode, which are quadratic functions of x and y for $N_\nu = N = 4$. In order to satisfy eqn (22) for the B_{1g} (B_{2g}) or A_{1g} modes, $m'' - m'$ has a component of $m'' - m' = \pm 1$ or $m'' - m' = 0$ for $m^{\mathrm{ph}} = \pm 1$ or 0, respectively. Such a situation is possible in the case that the m'' state is a virtual state that is expressed by a linear combination of the excited states.

In Table 5, we list σ_s for the A_{1g}, B_{1g}, and B_{2g} modes for a given incident circularly polarized light (σ_i) which satisfies eqn (24). As shown in Table 5, helicity-conserved A_{1g} Raman spectra can be observed for $\ell_i = 4p$, while helicity-changing B_{1g} or B_{2g} Raman spectra can be observed for odd numbers of ℓ_i. It is important to note that the B_{1g} or B_{2g} Raman spectra by non-vortex light ($\ell_i = 0$) are experimentally observed for 3D TaP[8] or 3D LaAlSi[9] which are comparable with the A_{1g} Raman spectra. It is not consistent with the results for B_{1g} or B_{2g} with $\ell_i = 0$ in Table 5. The reason for this inconsistency may come from the fact that the electron wavefunctions of the initial, intermediate and scattered states are not eigen function of D_{4h} since the optical transition occurs at the not-high-symmetry $\boldsymbol{k}$ point. Thus, several values of m are possible for the original wavefunction. Thus, we could not use the present result for 2D TaP or 2D LaAlSi Wyle semimetals.

5 Discussion and summary

In this paper, we have shown the selection rule for Raman spectra by using circularly-polarized vortex light for 2D materials with

Table 6 In the N rotational symmetry, possible values of orbital angular momentum of vector light ℓ are listed for spin angular momentum σ for the incident light that gives optical absorption σ_i, and for Raman scattered light σ_s with helicity-conserved phonon modes (A, $\sigma_s = \sigma_i$) and helicity-changing modes (E and B, $\sigma_s = -\sigma_i$). p is an integer

		σ_s	σ_s
N	σ_i	A	E, B
2	$\ell = 2p$	$\ell = 2p$[a]	$\ell = 2p$
3	Any ℓ[b]	$\ell = 3p$	$\ell = 3p$
4	$\ell \neq 4p + 2$	$\ell = 4p$	$\ell = 2p - 1$
6	$\ell = 2p$[c]	None[d]	$\ell = 2p$

[a] A_{1g} for $N = 2$ shows both the helicity-conserving and helicity-changing modes. [b] Only $\sigma_i = 1$ is possible for $\ell = 3p + 1$ and only $\sigma_i = -1$ is possible for $\ell = 3p - 1$. $\sigma_i = \pm 1$ is possible for $\ell = 3p$. [c] Only $\sigma_i = 1$ is possible for $\ell = 6p + 2$ and only $\sigma_i = -1$ is possible for $\ell = 6p - 2$. $\sigma_i = \pm 1$ is possible for $\ell = 6p$. [d] In graphene, there is no A mode.

N-fold ($N = 2$, 3, 4, and 6) rotational symmetry which is listed in Tables 2–5. In Table 6, we list the possible orbital angular momentum ℓ in the N fold rotational symmetry for given spin angular momentum of (1) incident light σ_i to have an optical absorption, (2) scattered light σ_s for helicity-conserved Raman mode (A) and helicity-exchanging Raman modes (E, B). When we compare the possible ℓ values for σ_i, the possible ℓ values depend on the sign of σ_i for $N = 3$ and 6, while not for $N = 2$ and 4. Possible ℓ values for σ_s are the same as those for σ_i for $N = 2$ and 6, while not for $N = 3$ and 4. Possible ℓ values for σ_s are the same as Np for $N = 2$ and 3 while not for $N = 4$ and 6. Thus for all four cases of N, the possible ℓ values have a behaviour independent of one another.

In order to get the results shown in the tables and the conservation rule of eqn (24), we need the following conditions: (1) the wavefunction of the initial, intermediate and final states should be an eigenfunction of N-fold rotation, (2) the electronic wavefunction is sufficiently delocalized in the 2D materials compared with the wavelength of light, and (3) the Raman tensor does not change shape in the presence of vortex light, which we will discuss below.

In the case of MoS_2, since the wavefunctions at the K and K' valley are eigenfunctions of L_z, valley polarization occurs, which gives non-trivial selection rules for vortex light as shown in Table 2. For most cases of 2D materials, however, since the optical absorption occurs at not high-symmetry $\boldsymbol{k}$ points such as the case of graphene or TaP, we do not expect the selection rule for the optical absorption matrix element. As a result, the selection rule of eqn (24) does not work perfectly. Nevertheless, in the case of graphene, since the optical absorption occurs near the K and K' points, the selection rule should be observed partially. It would be interesting to find 2D semiconductor materials whose optical absorption occurs at the high-symmetry $\boldsymbol{k}$ points. When we see the character tables of the point group, since the basis functions for C_{3h} and C_6 are expressed by either $(x + iy)^p$ or $(x - iy)^p$, $(p = 0, 1, 2)$ which are eigenfunctions of L_z, the optical selection rule for the vortex light would be interesting for such 2D materials.

When we obtain the selection rule of the optical absorption matrix element in eqn (21), we do not use the dipole approximation.

In the dipole approximation, we take the vector potential out of the matrix element by assuming that the vector potential changes very slowly compared with the spatial change of the wavefunction. In this case, the effect of the factor $\exp(-il\alpha)$ of the vortex light would not appear in eqn (21). Since the typical diameter of vortex light is in the order of the wavelength, we require condition (2) as shown above. It is important to note that the present selection rule cannot be used for a molecule since the molecular wavefunction is localized in the molecule.

In the case of 2D materials, since $r = \sqrt{x^2 + y^2}$ in the vector potential (eqn (10)) does not change by rotation around the z axis, the symmetry of the Raman tensor for vector light does not change even when we consider the vector potential for the vortex light as we discuss in Section 3.2. The shape of the Raman tensor will not change even for multi-layer 2D materials as long as the thickness is much smaller than the wavelength of the light. In this case, the phonon eigenmodes can be separated into either the in-plane of out-of-plane mode.

We hope that the selection rule will be observed experimentally for 2D materials which satisfy the above conditions.

Conflicts of interest

There are no conflicts to declare.

Acknowledgements

R. S. and M. S. U. acknowledge JSPS KAKENHI No. JP18H01810 and Center for Science and Innovations in Spintronics (CSIS) Tohoku University. N. T. H. acknowledges JSPS KAKENHI (Grant No. JP20K15178) and the financial support from the Frontier Research Institute for Interdisciplinary Sciences, Tohoku University. S. W. acknowledges the National Natural Science Foundation of China (Grant No. 11704165), the China Scholarship Council (Grant No. 201908320001) and the Natural Science Foundation of Jiangsu Province (Grant No. SBK2021020263).

Notes and references

1 M.-T. Gabriel, J. P. Torres and L. Torner, *Nat. Phys.*, 2007, **3**, 305.
2 W. Zhang, Q. Qi, J. Zhou and L. Chen, *Phys. Rev. Lett.*, 2014, **112**, 153601.
3 H. Kogelnik and T. Li, *Proc. IEEE*, 1966, **54**, 1312.
4 K. Toyoda, F. Takahashi, S. Takizawa, Y. Tokizane, K. Miyamoto, R. Morita and T. Omatsu, *Phys. Rev. Lett.*, 2013, **110**, 143603.
5 R. A. Beth, *Phys. Rev.*, 1936, **50**, 115.
6 Y. Tatsumi, T. Kaneko and R. Saito, *Phys. Rev. B*, 2018, **97**, 195444.
7 S. G. Drapcho, J. Kim, X. Hong, C. Jin, S. Shi, S. Tongay, J. Wu and F. Wang, *Phys. Rev. B*, 2017, **95**, 165417.
8 K. Zhang, X. Pang, T. Wang, F. Han, S.-L. Shang, N. T. Hung, A. R. T. Nugraha, Z.-K. Liu, M. Li, R. Saito and S. Huang, *Phys. Rev. B*, 2020, **101**, 014308.
9 K. Zhang, T. Wang, X. Pang, F. Han, S.-L. Shang, N. T. Hung, Z.-K. Liu, M. Li, R. Saito and S. Huang, *Phys. Rev. B*, 2020, **102**, 235162.
10 S.-Y. Chen, C. ZHeng, M. S. Fuhrer and J. Yan, *Nano Lett.*, 2015, **15**, 2526.
11 S. Zhang, N. Mao, N. Zhang, J. Wu, L. Tong and J. Zhang, *ACS Nano*, 2017, **11**, 10366.
12 R. Saito, M. Hofmann, G. Dresselhaus, A. Jorio and M. S. Dresselhaus, *Adv. Phys.*, 2011, **60**, 413.
13 A. Jorio, M. S. Dresselhaus, R. Saito and G. Dresselhaus, *Raman Spectroscopy in Graphene Related Systems*, Wiley-VCH Verlag GmbH & Co KGaA, WeinHeim, Germany, 2010, p. 368.
14 Y. Tatsumi and R. Saito, *Phys. Rev. B*, 2018, **97**, 115407.
15 S. Ishii, N. Yokoshi and H. Ishihara, *J. Phys.: Conf. Ser.*, 2019, **1220**, 012056.
16 J. Li, J. J. Tu and J. L. Birman, *J. Phys. Chem. Solids*, 2015, **77**, 117.
17 A. Grüneis, R. Saito, G. G. Samsonidze, T. Kimura, M. A. Pimenta, A. Jorio, A. G. S. Filho, G. Dresselhaus and M. S. Dresselhaus, *J. Phys. Chem. Solid*, 2003, **67**, 165402.
18 R. Saito, Y. Tatsumi, S. Huang, X. Ling and M. S. Dresselhaus, *J. Phys.: Condens. Matter*, 2016, **28**, 353002.
19 M. Beijersbergen, R. Coerwinkel, M. Kristensen and J. Woerdman, *Opt. Commun.*, 1994, **112**, 321.
20 K. F. Mak, K. He, J. Shan and T. F. Heinz, *Nat. Nanotechnol.*, 2012, **7**, 494.
21 H. Zeng, J. Dai, W. Yao, D. Xiao and X. Cui, *Nat. Nanotechnol.*, 2012, **7**, 490.
22 T. Cao, G. Wang, W. Han, H. Ye, C. Zhu, J. Shi, Q. Niu, P. Tan, E. Wang, B. Liu and J. Feng, *Nat. Commun.*, 2012, **3**, 887.
23 A. M. Jones, H. Yu, N. J. Ghimire, S. Wu, G. Aivazian, J. S. Ross, B. Zhao, J. Yan, D. G. Mandrus, D. Xiao, W. Yao and X. Xu, *Nat. Nanotechnol.*, 2013, **8**, 634.
24 R. Suzuki, M. Sakano, Y. J. Zhang, R. Akashi, D. Morikawa, A. Harasawa, K. Yaji, K. Kuroda, K. Miyamoto, T. Okuda, K. Ishizaka, R. Arita and Y. Iwasa, *Nat. Nanotechnol.*, 2014, **9**, 611.
25 S. Wu, J. S. Ross, G.-B. Liu, G. Aivazian, A. Jones, Z. Fei, W. Zhu, D. Xiao, W. Yao, D. Cobden and X. Xu, *Nat. Phys.*, 2013, **9**, 149.
26 K. Ghalamkari, Y. Tatsumi and R. Saito, *J. Phys. Soc. Jpn.*, 2018, **87**, 024710.
27 H. Zeng, J. Dai, W. Yao, D. Xiao and X. Cui, *Nat. Nanotechnol.*, 2012, **7**, 490.
28 D. Xiao, G.-B. L. nad Wanxiang Feng, X. Xu and W. Yao, *Phys. Rev. Lett.*, 2012, **108**, 196802.
29 A. Grüneis, R. Saito, G. G. Samsonidze, T. Kimura, M. A. Pimenta, A. Jorio, A. G. S. Filho, G. Dresselhaus and M. S. Dresselhaus, *J. Phys. Chem. Solid*, 2003, **67**, 165402.
30 X. Ling, S. Huang, E. H. Hasdeo, L. Liang, W. M. Parkin, Y. Tatsumi, A. R. T. Nugraha, A. A. Puretzky, P. M. Das, B. G. Sumpter, D. B. Geohegan, J. Kong, R. Saito, M. Drndic, V. Meunier and M. S. Dresselhaus, *Nano Lett.*, 2016, **16**, 2260.
31 N. Mao, S. Zhang, J. Wu, H. Tian, J. Wu, H. Xu, H. Peng, L. Tong and J. Zhang, *Nano Res.*, 2018, **11**, 3154.
32 F. Xia, H. Wang and Y. Jia, *Nat. Commun.*, 2014, **5**, 4458.
33 Y. Takao and A. Morita, *Phys. B*, 1981, **105**, 93.

